〔Articles〕

Tension of Infinite Solids Containing Periodic Arrays of Rigid Short Flat Inclusions

Hidenobu IGAWA*

Abstract:

A rectangular array and a zig-zag array of rigid short flat inclusions in an infinite solid subjected to biaxial tension are considered in this paper. In the analyses, we take a rectangular unit region and a triangular unit region, and express complex stress potentials by eigen-function expansions in forms satisfying the continuity relations along the inclusion boundaries. The unknown coefficients are determined from the boundary conditions in the unit regions which are expressed in terms of the resultant forces and displacements. Numerical calculations are carried out for various combinations of inclusion length and inclusion space. The stress intensity factor and the tensile stiffness for the solids that contain inclusions are represented in figures. The results of the tensile stiffness are fitted to polynomial formulae. They are useful to the design of the composite materials.

1. Introduction

Nowadays composite materials that consist of reinforced fibers dispersed in plastic materials are being used in mechanical structures. These materials are in great demand as industrial products for light weighting and high strength. However, rational techniques based on mechanical analyses have not contributed to the design to any great extent.

Theoretical analyses on rigid short flat inclusions have been made by some researchers[1-4]. They were analyzed on two or three inclusions in an infinite solid. The authors have studied on multiple cracks, elliptical holes and circular inclusions[5-9]. The authors' methods were useful for analyzing these problems.

This paper is concerned with theoretical analyses of periodic arrays of rigid short flat inclusions in solids under biaxial tension. In the analyses, we chose suitable unit regions, and express complex stress potentials by eigen-function expansions in forms satisfying the continuity relations along the inclusion boundaries. The unknown coefficients are determined from the boundary conditions of the unit regions. At this stage, we use a procedure based on the element-wise resultant forces and displacements in order to get highly accurate results.

Calculations are carried out for various inclusion sizes and inclusion spaces both vertical to and parallel to the load. Numerical results of the stress intensity factor and the tensile stiffness for the solids that contain the inclusions are given for various parameters. The results of the tensile stiffness are then fitted to polynomial formulae for the convenience of engineering applications.

2. Theoretical analysis

2.1 Complex stress potentials

In plane problems of elasticity, the Cartesian components of stress, resultant force and displacement are given

* Department of Mechanical Systems Engineering
平成18年4月11日受理

in terms of two complex potentials $\phi(z)$, $\Omega(z)$ as follows:

$$\sigma_x+\sigma_y=4\mathrm{Re}[\phi(z)],\quad \sigma_x-\sigma_y-i\tau_{xy}=2[\phi(z)-\bar{\Omega}(z)+2iy\phi'(z)] \tag{1}$$

$$P_y+iP_x=-\int\bar{\phi}(\bar{z})d\bar{z}-\int\bar{\Omega}(z)dz+2iy\phi(z) \tag{2}$$

$$2G(u+iv)=\varkappa\int\bar{\phi}(\bar{z})d\bar{z}-\int\bar{\Omega}(z)dz+2iy\phi(z). \tag{3}$$

where G is the shear modulus and $\varkappa$ is defined by Poisson's ratio ν as

$$\varkappa=(3-\nu)/(1+\nu)\ \text{(plane stress)},\quad 3-4\nu\ \text{(plane strain)}. \tag{4}$$

This paper deals with the following two typical distributions of short inclusions in an infinite solid subjected to biaxial tension:

Problem (a): Rectangular array of rigid short flat inclusions (Fig. 1(a))

Problem (b): Zig-zag array of rigid short flat inclusions (Fig. 1(b))

The x- and y-axes are taken with their origin at the center of one of the inclusions as shown by Figs. 1(a) and 1(b). In both the problems, a is the half-length of the inclusions and b, c are the inclusion spaces in the x, y-directions. These solids are subjected to average tensile stresses σ_1, σ_2 in the x- and y-directions.

In the analyses, we take a rectangular unit region ODHKO for the problem (a) shown in Fig. 2 and a triangular unit region ODFO for the problem (b) shown in Fig. 3. We express the complex potentials in these unit regions by the following eigen-function expansions:

$$\phi(z)=\sum_{n=1}^{\infty}\left(A_n\frac{z^{2n-1}}{\sqrt{z^2-a^2}}+B_nz^{2n-2}\right),\quad \Omega(z)=-\varkappa\sum_{n=1}^{\infty}\left(A_n\frac{z^{2n-1}}{\sqrt{z^2-a^2}}-B_nz^{2n-2}\right) \tag{5}$$

where A_n and B_n are real coefficients.

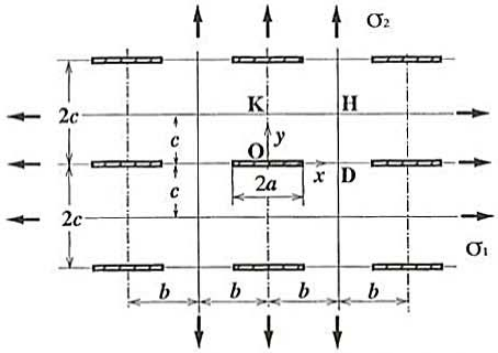

Fig. 1(a) Rectangular array of rigid short flat inclusions

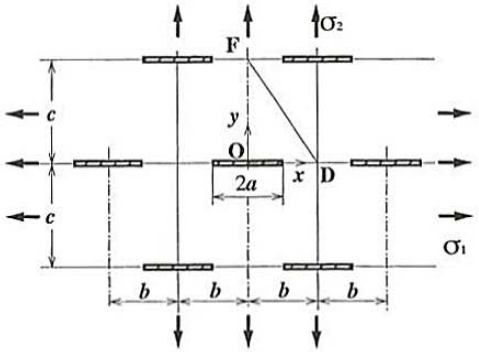

Fig. 1(b) Zig-zag array of rigid short flat inclusions

2.2 Determination of unknowns

Complex potentials (5) satisfy not only the symmetry conditions along x- and y-axes, but also the continuity conditions for stress and displacement along the rigid inclusion boundary. Therefore, the unknown coefficients A_n and B_n must be determined only from the boundary conditions along the outer edges of the unite regions[5,10].

In the numerical calculation, we use a new technique based on element-wise resultant forces and displacements. The procedures for both the problems are described below.

(a) Rectangular array of rigid short flat inclusions

We divide the sides DH and HK of the rectangular unite region into N_1 and N_2 equal intervals, respectively. These intervals are, Q_1Q_2, Q_2Q_3, ⋯ and Q_NQ_{N+1} as shown in Fig. 2, where $N=N_1+N_2$.

Side DH:

The stress state is symmetric about DH. Then τ_{xy} vanishes and u is constant along DH. These conditions are

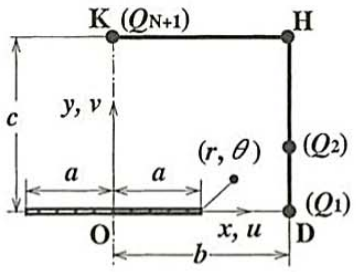

Fig. 2 Rectangular unit region

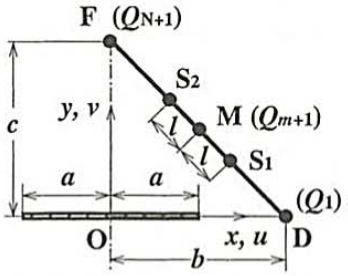

Fig. 3 Triangular unit region

replaced by the following relations in terms of Py and u for each of the intervals:

$$[P_y]_j=0 \quad (j=1, 2, \cdots, N_1)$$
$$[u]_{j+1}-[u]_j=0 \quad (j=1, 2, \cdots, N_1-1) \tag{6}$$

where j is the interval number.

$[P_y]_j$ is given from the real part of Eq. (2) by taking the difference between $P_{y,Q_{j+1}}$ and P_{y,Q_j} at the two points Q_{j+1} and Q_j, and $[u]_j$ is defined as the mean of u at Q_{j+1} and Q_j which are obtained from the real part of Eq. (3). These lead to the relationships as followings,

$$[P_y]_j=P_{y,Q_{j+1}}-P_{y,Q_j}$$
$$[u]_j=(u_{Q_{j+1}}+u_{Q_j})/2 \quad (j=1, 2, \cdots, N_1). \tag{7}$$

Side HK:

The stress state is symmetric about side HK, and we have the following relations similar to Eq. (6):

$$[P_x]_j=0 \quad (j=N_1+1, N_2+2, \cdots, N)$$
$$[v]_{j+1}-[v]_j=0 \quad (j=N_1+1, N_2+2, \cdots, N-1) \tag{8}$$

where $[P_x]_j$, $[v]_j$ are defined as

$$[P_x]_j=P_{x,Q_{j+1}}-P_{x,Q_j}$$
$$[v]_j=(v_{Q_{j+1}}+v_{Q_j})/2 \quad (j=N_1+1, N_2+2, \cdots, N). \tag{9}$$

Furthermore, the resultant forces along DH, HK should balance the external loads, and we have

$$[P_x]_D^H=\sigma_1 c, \quad [P_y]_H^K=\sigma_2 b. \tag{10}$$

(b) Zig-zag array of rigid short flat inclusions

We divide the side DF of the triangular unite region into N equal intervals, respectively. These intervals are Q_1Q_2, Q_2Q_3, $\cdots$ and Q_NQ_{N+1} as shown in Fig. 3, where $N=2m$.

Referring to Fig. 3, let M be the midpoint of the side DF in the triangular unit region ODFO. So the stress field is symmetric about point M, and any two points S_1 and S_2 on DF which are equidistant from $M(Q_{m+1})$ must be in the same stress state, and displacements of these points relative to M must be the same. These boundary conditions are replaced by the following relations:

$$[P_x]_{Q_t}^{Q_{m+1}}=[P_x]_{Q_{m+1}}^{Q_{2m+2-t}}, \quad [P_y]_{Q_t}^{Q_{m+1}}=[P_y]_{Q_{m+1}}^{Q_{2m+2-t}} \quad (t=1, 2, \cdots, m;\ m=N/2) \tag{11}$$
$$[u]_{Q_t}^{Q_{m+1}}=[u]_{Q_{m+1}}^{Q_{2m+2-t}}, \quad [v]_{Q_t}^{Q_{m+1}}=[v]_{Q_{m+1}}^{Q_{2m+2-t}} \quad (t=1, 2, \cdots, m;\ m=N/2). \tag{12}$$

Furthermore, the resultant forces along the outer edge of the unit region should balance the external loads, and we have

$$[P_x]_D^F=\sigma_1 c, \quad [P_y]_D^F=\sigma_2 b. \tag{13}$$

Thus we have $2N$ relations (6), (8), (10) for the problem (a), and $(2N+1)$ relations (11), (12), (13) for the problem (b). Corresponding to these relations, we take $2N$ unknowns $A_n(n\leq N)$, $B_n(n\leq N)$ for the problem (a) and $(2N+1)$ unknowns $A_n(n\leq N+1)$, $B_n(n\leq N)$ for the problem (b) neglecting higher order coefficients, and these unknowns are determined from the corresponding boundary conditions shown above.

2.3 Stress state around the rigid inclusion tips

The stresses around the rigid inclusion tips are obtained as follows[2,3]:

$$\sigma_x=\frac{f}{\sqrt{2r}}\cos\frac{\theta}{2}\left\{\frac{3+\varkappa}{2}-\sin\frac{\theta}{2}\sin\frac{3}{2}\theta\right\}$$

$$\sigma_y=-\frac{f}{\sqrt{2r}}\cos\frac{\theta}{2}\left\{\frac{\varkappa-1}{2}-\sin\frac{\theta}{2}\sin\frac{3}{2}\theta\right\}$$

$$\tau_{xy}=\frac{f}{\sqrt{2r}}\sin\frac{\theta}{2}\left\{\frac{1+\varkappa}{2}-\cos\frac{\theta}{2}\cos\frac{3}{2}\theta\right\} \tag{14}$$

where stress intensity factor f is found in the complex potential $\phi(z)$ as follow:

$$f=2\sqrt{2}\lim_{z\to a}[\sqrt{z-a}\,\phi(z)]. \tag{15}$$

3. Numerical results and discussion

3.1 Physical quantities and accuracy of results

Numerical results of the treated problems depend upon the ratio of a, b, c. We define the following parameters:

$$\lambda=\frac{a}{b},\quad \gamma=\frac{c}{b},\quad \mu=\frac{b}{c}=\gamma^{-1}. \tag{16}$$

In the present problem, we are especially interested in two quantities. One is the stress intensity factor, and the other is the effect of inclusions on the apparent tensile stiffness of the solid. For these quantities, dimensionless factors are defined by the following equations:

Dimensionless stress intensity factor:

$$F=\frac{f}{\sigma\sqrt{a}},\quad \sigma=\sigma_1 \text{ or } \sigma_2. \tag{17}$$

Tensile stiffness factor:

$$C_x=\frac{E_x^*}{E_0},\quad C_y=\frac{E_y^*}{E_0}$$

E_x^*, E_y^*=apparent Young's modulus of solid with inclusions in x- and y- directions

E_0=Young's modulus of material

$=E$ (plane stress), $E/(1-\nu^2)$ (plane strain) (18)

where E is the Young's modulus of the material measured with thin plate specimens.

Numerical results from the present analyses are expected to approach the exact values with increasing numbers of the boundary elements on the unit region, or N. As an example, Table 1 gives F and C_x for the case of $c/b=1$, $a/b=0.5$, ($\sigma_1=\sigma$, $\sigma_2=0$) with various values of N in the problems (a) and (b). We find convergence of the results with increasing division numbers N. Both the problems (a) and (b) are calculated for the plane strain case. The procedure as shown in Table 1 has been taken to confirm high accuracy of all the numerical results, which is

Table 1 Variations of results with division numbers

N	Problem (a) [$c/b=1$, $a/b=0.5$, ($\sigma_1=\sigma$, $\sigma_2=0$), rectangular unit region]		Problem (b) [$c/b=1$, $a/b=0.5$, ($\sigma_1=\sigma$, $\sigma_2=0$), triangular unit region]	
	$F\left(=\frac{f}{\sigma_1\sqrt{a}}\right)$	C_x	$F\left(=\frac{f}{\sigma_1\sqrt{a}}\right)$	C_x
8	0.39417	1.11994	0.34645	1.23017
12	0.39334	1.12083	0.34645	1.23115
24	0.39331	1.12092	0.34645	1.23115
36	0.39331	1.12094	0.34645	1.23115

discussed in the following section.

3.2 Numerical results

Numerical values of F subjected to tensile stress σ_1 in the x-direction for the problems (a) and (b) are plotted with solid curves in Figs. 4(a) and 4(b), respectively.

In the case of $\lambda \to 0$, f is the stress intensity factor for a single rigid flat inclusion in a wide plate subjected to tensile stress σ_1, and F is given by the explicit form

$$[F]_{\lambda\to 0}=\frac{[f]_{\lambda\to 0}}{\sigma_1\sqrt{a}}=\frac{1+\chi}{4\chi}. \tag{19}$$

In both the problems, the trend of increasing or decreasing F with increasing λ varies depending on the values of c/b.

Tensile stiffness factors C_x and C_y defined by Eq. (18) have been calculated for various values of c/b and λ. The results for both the problems are plotted with solid curves in Figs. 5(a)-6(b). C_x and C_y monotonically increase with increasing values of λ. C_x, λ-curves shown in Figs. 5(a) and 5(b) rise with decreasing values of c/b which indicate the ratio of space between up and down inclusions.

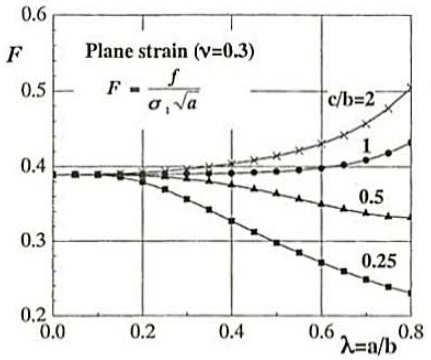

Fig. 4(a) F, λ-relations for Problem (a) ($\sigma_1=\sigma$, $\sigma_2=0$)

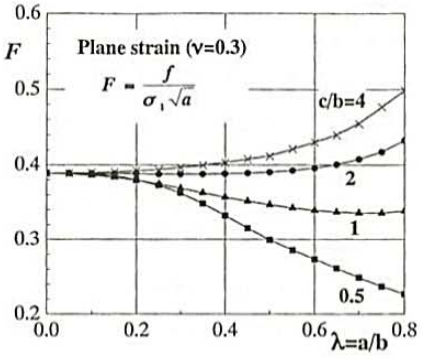

Fig. 4(b) F, λ-relations for Problem (b) ($\sigma_1=\sigma$, $\sigma_2=0$)

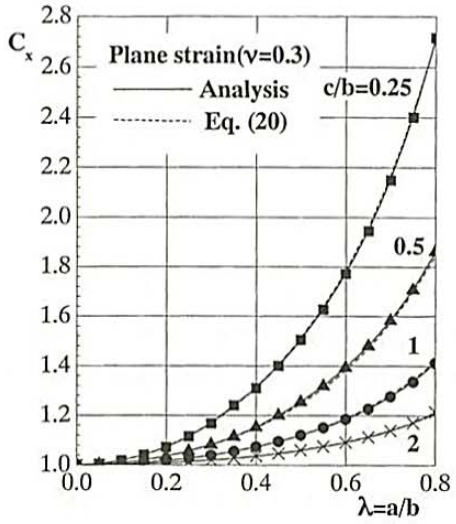

Fig. 5(a) C_x, λ-relations for Problem (a) ($\sigma_1=\sigma$, $\sigma_2=0$)

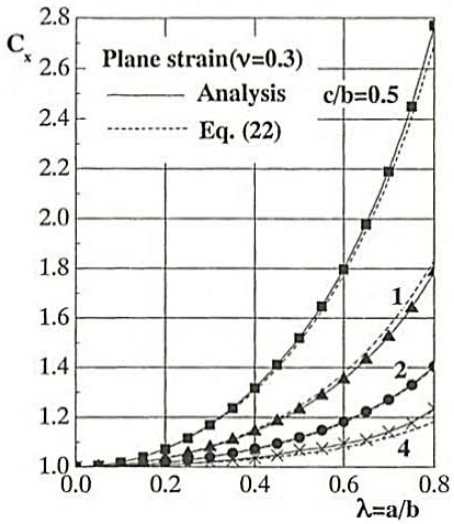

Fig. 5(b) C_x, λ-relations for Problem (b) ($\sigma_1=\sigma$, $\sigma_2=0$)

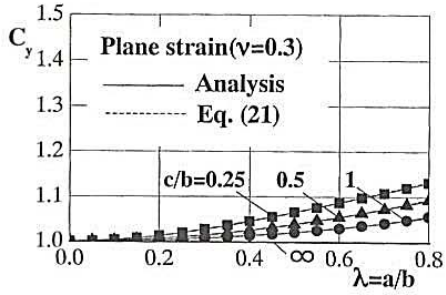

Fig. 6(a) C_y, λ-relations for Problem (a) ($\sigma_1=\sigma$, $\sigma_2=0$)

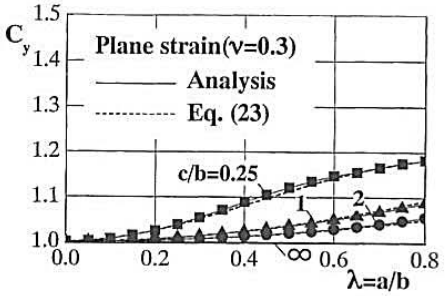

Fig. 6(b) C_y, λ-relations for Problem (b) ($\sigma_1=\sigma$, $\sigma_2=0$)

3.3 Formulae of the tensile stiffness

In the above, we calculated the tensile stiffness factors C_x and C_y for various combinations of λ and μ. However, when the values for some other cases are required, we have to make interpolations with respect to two parameters, causing considerable errors in the results.

We have fitted a power series to analytical values of C_x and C_y for both the problems[9], and the following formulae are obtained:

(a): Rectangular array of rigid short flat inclusions (Fig. 1(a))

In the case subjected to tension ($\sigma_1=\sigma$, $\sigma_2=0$) in the x-direction,

$$C_x=1+\lambda^2[0.0213-0.3889\lambda+1.114\lambda^2-0.8354\lambda^3+\mu(0.4066+0.4569\lambda-1.1357\lambda^2+1.2173\lambda^3)]$$

(range of $0.25\leq\mu\leq4$ and $\lambda\leq0.8$; mean error 0.2%). (20)

In the case subjected to tension ($\sigma_1=0$, $\sigma_2=\sigma$) in the y-direction,

$$C_y=1+\lambda^2\mu[0.0728+0.0326\lambda+\mu(0.0036-0.0193\lambda)]$$

(range of $0\leq\mu\leq4$ and $\lambda\leq0.8$; mean error 0.04%). (21)

(b): Zig-zag array of rigid short flat inclusions (Fig. 1(b))

In the case subjected to tension ($\sigma_1=\sigma$, $\sigma_2=0$) in the x-direction,

$$C_x=1+\lambda^2[0.0082-0.1391\lambda-0.0350\lambda^2+0.1453\lambda^3+\mu(0.8191+0.6045\lambda-1.1128\lambda^2+1.4892\lambda^3)]$$

(range of $0.25\leq\mu\leq2$ and $\lambda\leq0.8$; mean error 0.8%). (22)

In the case subjected to tension ($\sigma_1=0$, $\sigma_2=\sigma$) in the y-direction,

$$C_y=1+\lambda^2\mu[0.1438+0.0325\lambda+\mu(0.0100-0.0434\lambda)]$$

(range of $0\leq\mu\leq4$ and $\lambda\leq0.8$; mean error 0.2%). (23)

Eqs. (20) to (23) give practically exact values, as see from the mean percent errors shown in parentheses with each of the formulae. The values for these equations are plotted in Figs. 5(a) to 6(b) with dashed curves, showing close agreement with the analytical curves.

4. Conclusions

(1) We considered a rectangular array and a zig-zag array of rigid short flat inclusions in an infinite solid subjected to biaxial tension. In the analyses, we took a rectangular unit region and a triangular unit region, and expressed the complex stress potentials in eigen-function expansions in forms satisfying the continuity relations along the inclusion boundaries. The unknown coefficients were determined from the boundary conditions of the unit regions which were expressed in terms of resultant forces and displacements.

(2) Numerical calculations were carried out for various combinations of a/b and c/b, where a, b and c were the half-length of the inclusions and the inclusion spaces in the x, y-directions. The stress intensity factor and the tensile stiffness for the solids that contain the inclusions were represented in the figures by dimensionless quantities F, and

C_x and C_y.

(3) The results of the tensile stiffness were fitted to reliable polynomial formulae. They are useful to the design of the composit materials.

REFERENCES

[1] P.K. Mallick, *Fiber-reinforced composites,* Marcel Dekker, Inc., pp.91-189.

[2] F. Erdogan, G.D. Gupta, *Stresses near a flat inclusion in bonded dissimilar materials,* Int J. Solids Structures 8 (1972), pp.533-547.

[3] C. Atkinson, *Some ribbon-like inclusion problems,* Int. J. Engng. Sci. 11 (1973), pp243-266.

[4] Y.K. Cheung, Y.Z. Chen, *Multiple rigid line problem in an infinite plate,* Engg. Frac. Mech., Vol.34 (1989), pp. 379-391.

[5] M. Isida, H. Igawa, *Doubly-periodic array and zig-zag array of cracks in solids under uniaxial tension,* Int. J. Frac. Mech. 53 (1992), pp.249-260.

[6] H. Igawa, *Tension of an infinite solid containing a doubly-periodic array of slant cracks,* Boundary Element Technology XIII, WIT Press (1999), pp.567-575.

[7] H. Igawa, *In-plane shear of an infinite solid containing a doubly-periodic array of slant cracks,* Boundary Element Technology XIII, WIT Press (1999), pp.609-618.

[8] H. Igawa, *Rectangular array and zig-zag array of elliptical holes in solids under uniaxial tension,* Kye Engineering Materials Vols.183-187, Trans Tech Publications (2000), pp.25-30.

[9] M. Isida, H. Igawa, *Analysis of a zig-zag array of circular inclusions in a solid under uniaxial tension,* Int. J. Solids Structures 27 (1991), pp.1515-1535.

[10] M. Isida, *Effect of width and length on stress intensity factors of internally cracked plates under various boundary conditions,* Int. J. Frac. Mech. 7 (1971), pp.301-316.

[11] H. Igawa, T. Hirano, A. Kumabe, *Tension of infinite solids containing periodic arrays of rigid flat inclusions,* Bulletin of Kurume Institute of Technology No.23 (1999), pp.1-6.

[12] H. Igawa, *Tension of infinite solids containing periodic arrays of rigid short flat inclusions,* 2nd China-Europe Symposium on Processing and Properties of Reinforced Polymers (Beijing, China 2005), (Oral presentation).